PCCP

Kinetic study in a microwave-induced plasma afterglow of the Fe (a $^5D_4$) reaction with NO_2 from 303 to 814 K

C. Vinckier* and K. Cappan

Laboratory for Physical and Analytical Chemistry, K.U. Leuven, Celestijnenlaan 200F, B-3001, Leuven, Belgium. E-mail: Chris.Vinckier@chem.kuleuven.ac.be

Received 11th July 2003, Accepted 28th October 2003
First published as an Advance Article on the web 14th November 2003

A kinetic study of the reaction of ground state Fe atoms (a $^5D_4$) with NO_2 has been performed in a fast-flow reactor. A microwave-induced plasma afterglow system with H atoms reacting with the gaseous Fe_xCl_{3x}(g) oligomers was used as Fe atom source. The Fe atoms were monitored by atomic absorption spectroscopy (AAS) at 248.3 nm. The rate constant k_1 of the reaction Fe + NO_2 → products has been determined at temperatures between 303 and 814 K and was found to be equal to $k_1 = (4.8^{+0.7}_{-0.6}) \times 10^{-10}\exp(-(4.5 \pm 0.4)/RT$ kJ mol^{-1}) cm^3 molecule^{-1} s^{-1}. The mechanistic implications in terms of the "electron-jump" mechanism are also discussed and it was concluded that the concept of "harpooning" is not applicable to reaction (1). Instead, the value of k_1 can remarkably well be simulated in terms of the simple gas kinetic collision model.

Introduction

The introduction of the high-temperature fast-flow reactor (HTFFR) technique by A. Fontijn *et al.* has allowed the determination of a large number of kinetic parameters of refractory metal atom-gas reactions over a wide temperature range between 300 and 2000 K.[1] More recently, the high-temperature photochemistry (HTP) technique[2] has been developed as an alternative metal atom source. While with the former technique metal atoms were mostly generated by thermal heating of the metal, with the HTP-technique metal atoms were produced photolytically and were monitored in a real time detection mode.

If one restricts metal atom sources to Fe atoms, pulsed photolysis of a suitable Fe atom precursor is most commonly used in gas phase kinetic studies. Likely candidates are volatile compounds such as organo-metal[3–5] or metal carbonyl compounds.[6] In most cases one has a pseudo-static system where the characteristic time scale of the reaction is in the range of a fraction of milliseconds compared to the residence time of the reagents in the cell which can be of the order of seconds. In some cases a hollow cathode sputtering technique was used in combination with a fast-flow reactor.[7]

An alternative method to vaporise non-volatile metals is the plasma-afterglow atomisation technique[8] where metals in the gas phase were formed by a reaction of a metal salt with hydrogen atoms in a fast-flow reactor. It was shown that $FeCl_3$(s) is a sufficiently volatile Fe salt to generate high enough Fe atom precursor concentrations leading ultimately to the formation of Fe atoms.[9] This technique will now be applied to a kinetic study of the reaction between Fe atoms and nitrogen dioxide in the temperature range from 303 to 814 K:

$$\text{Fe (a } {}^5D_4) + NO_2 \rightarrow \text{products} \qquad \text{(r.1)}$$

The Arrhenius expression for k_1 will be derived and compared with the recent measurements by Plane *et al.*[10] who have investigated the same reaction in a somewhat lower temperature interval between 192 and 471 K. The magnitude of k_1 will also be compared with the calculated value on the basis of the gas kinetic collision model.

Experimental technique

The experimental technique was basically the same as used for our kinetic studies of the Cu atom reactions[12,13] and it has recently been described for the generation of Fe atoms.[9] It consisted of a quartz fast-flow reactor with an internal diameter of 5.7 cm and a length of 1 m. The water cooled flange at the upstream end carried a carrier gas inlet and the sample holder with an external diameter of 1.9 cm. A Kanthal resistance wire allowed the solid $FeCl_3$(s) pellet to be heated up to a temperature T_s in the range between 300 and 800 K, independently of the reactor temperature. A shielded chromel–alumel thermocouple in contact with the $FeCl_3$(s)-pellet monitored the temperature T_s of the solid. Hydrogen atoms were produced by a microwave-induced plasma in molecular hydrogen/argon mixtures. Therefore a second gas inlet was equipped with an air cooled microwave cavity type 216 L powered by an Electro Medical Supplies microwave generator operating at 2450 ± 25 MHz and with a maximum power of 200 Watt. Between the cavity and the reactor a Wood's horn trapped the UV light produced by the plasma. The reactor oven allowed the gas temperature, T_g, to be varied between 300 and 1000 K. Constant temperatures could be maintained within 2.5% over a distance of *ca.* 25 cm.

At the downstream end the water-cooled flange carried two quartz probes: an on-axis movable tube containing a thermocouple to measure the gas temperature T_g and the additive inlet for the introduction of the reagent, in this case nitrogen dioxide.

An Alcatel type 2033 double-stage oil rotary pump with a nominal pump capacity of 33 m^3 h^{-1} resulted in a flow velocity for argon of (326 ± 4) cm s^{-1} at 295 K. Pressures were measured by means of a Datametrics type 1018 electronic manometer powering a sensor which covered pressures from 1.3×10^{-1} to 1.7×10^3 Pa.

In the kinetic zone the Fe atoms were detected by atomic absorption spectroscopy (AAS) at 248.3 nm. The light path of the hollow cathode lamp was focussed perpendicular to the main reactor axis through a slit of 1 cm in the reactor oven

construction. The light exiting the reactor was then focussed on the entrance slit of a McPherson model 270 monochromator which contains a diffraction grating with 1200 lines mm^{-1} and has a reciprocal dispersion of 2.0 nm mm^{-1}. A Hamamatsu R955 photonmultiplier with a wavelength range from 160 to 900 nm was used as detector. While the detection system remained at a fixed position, the fast-flow reactor assembly was mounted on a carriage which allowed a horizontal displacement so that the Fe absorbances (A_{Fe}) could be measured along the reactor axis. The detection limit for Fe atoms at $A_{Fe} = 0.005$ was estimated to be 1.3×10^9 atoms cm^{-3} at 300 K.[9]

The gases used were argon from Messer with a purity better than 99.999%. Hydrogen is from L'Air Liquide with a quality of 99.9997%. Nitrogen dioxide was added as a 0.117% mixture in UPH helium (UCAR). Gas flows were regulated *via* Brooks precision needle valves of the ELF type and mass flow controllers type 5850E. The iron salt $FeCl_3 \cdot 6H_2O$ from Riedel de Haën had purity >99%.

Results and discussion

Microwave-induced plasma afterglow atomisation of $FeCl_3$(s)

The major characteristics of the microwave-induced plasma afterglow atomisation of $FeCl_3$(s) have been discussed in more detail recently.[9] In principle, the iron chloride oligomers Fe_xCl_{3x}(g) produced by the vaporisation of the $FeCl_3$(s)-pellet were mixed with the hydrogen atoms from the microwave-induced plasma. A complex and yet unknown reaction sequence converts a fraction of Fe_xCl_{3x}(g) into Fe atoms through subsequent atomic hydrogen reactions:

$$Fe_2Cl_3(g) + 3H \rightarrow \ldots \rightarrow Fe(g) + 3HCl \qquad (r.2)$$

$$Fe_2Cl_6(g) + 6H \rightarrow \ldots \rightarrow 2Fe(g) + 6HCl \qquad (r.3)$$

These processes seemed to be fast enough to generate maximum Fe atom concentrations of about 5×10^{10} atoms cm^{-3} which were sufficiently high not only to be measured by AAS but also to perform kinetic studies.

The Fe atom concentration reached its maximum within a time scale of less than 30 ms which corresponded to a distance of *ca.* 10 cm downstream of the plasma inlet. Further downstream, A_{Fe} started to decrease due to the loss process of the Fe atoms on the reactor wall. Since one can assume that the sticking coefficient γ_{Fe} on the reactor wall approaches unity, the decay of the Fe atoms will be diffusion controlled and the observed decay constant k_{loss} can be expressed as:[14–16]

$$k_{loss} = \frac{7.34 D_{Fe/Ar}}{2R^2} \qquad (1)$$

where $D_{Fe/Ar}$ is the binary diffusion coefficient of Fe atoms in argon and R is the reactor radius. From 58 measurements of k_{loss} under a wide variety of experimental conditions, $D_{Fe/Ar} = (3.1 \pm 0.1) \times 10^4$ cm^2 s^{-1} Pa could be derived at 303 K.[9]

The reaction between Fe atoms and NO_2

The rate constant k_1 could now be determined from the Fe atom decay as a function of the reaction time when various amounts of nitrogen dioxide were added. The mathematical treatment to describe the evolution of A_{Fe} as a function of the reaction time is the same as used in our previous kinetic studies of the Cu/NO_2[12] and Cu/methyl halide reactions:[13]

$$\ln(A_{Fe}) = -\left(\frac{k_1[NO_2]}{\eta} + \frac{7.34 D_{Fe/Ar}}{2R^2}\right) t + B \qquad (2)$$

in which t is the reaction time, B an integration constant and η a correction factor. A complete analysis of possible errors in flow tube measurements and the influence of the various flow characteristics on the magnitude of η is already presented in earlier publications.[1,17,18]

The value of k_1 will be determined by following A_{Fe} as a function of the reaction time t at various amounts of added NO_2. When the slopes $S = k_1/\eta$ of eqn. (2) were plotted *versus* $[NO_2]$, straight lines should be obtained. For measurements in argon where mixing times exceed the representative residence times in flow reactors of *ca.* 1 m length, the correction factor η was set equal to 1.3 with an associated systematic error of 10%.[1] All plots and calculations were made using the SAS-607 statistical package[19] and the quoted uncertainties are given as 1σ standard deviations.

As an example to illustrate the procedure used, the natural logarithm ln A_{Fe} was plotted *versus* the reaction time for various $[NO_2]$ at a gas temperature $T_g = 303$ K (Fig. 1). Two blank runs were performed in the absence of NO_2, one at the start and one at the end of the experiment.

The reactor pressure P_r was 1.3×10^3 Pa and the other parameters were set at $T_s = 391$ K and $[H_2] = 6.0 \times 10^{-1}$ Pa. Experimental conditions were adjusted to have maximum Fe-absorbances of 0.05 in the kinetic zone corresponding to initial Fe atom concentrations of *ca.* 1×10^{10} atoms cm^{-3}.

When the slope S of these lines was plotted *versus* $[NO_2]$, fairly good straight lines were obtained as is illustrated in Fig. 2 for three different temperatures: 300, 447 and 814 K.

From these slopes, rate constants of respectively 8 ± 2, 15 ± 6 and 23 ± 19 each expressed in 10^{-11} cm^3 $molecule^{-1}$ s^{-1} could be derived.

Influence of the microwave-induced plasma afterglow parameters

In order to verify that the characteristics of the plasma afterglow had no effect on the magnitude of the derived rate constants, various parameters such as the temperature of the $FeCl_3$(s)-pellet, the hydrogen content and reactor pressure have been varied and their influence on k_1 checked. The experimental conditions are summarised in Tables 1 and 2. One can see that varying T_s between 384 and 418 K had no systematic effect on of k_1 at 303 K. This implies that increasing precursor concentrations of $FeCl_3$(g) and Fe_2Cl_6(g) by a factor of 10 and more[9] did not measurably affect k_1. This proves that once the Fe atoms were formed, subsequent reactions with these compounds were unimportant.

The influence of the molecular hydrogen concentration in the discharge has also been checked. At 3.1×10^{-1} Pa H_2 the average value of k_1 was equal to 6.9 ± 0.8, while at 6.0×10^{-1} Pa H_2 the value of 6.5 ± 1.4 was found, each

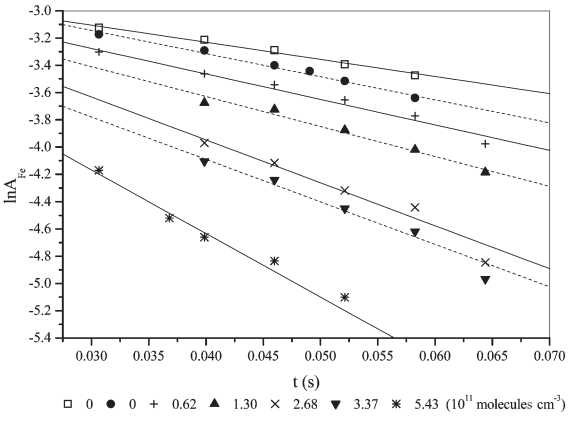

Fig. 1 Natural logarithm of the Fe absorbance lnA_{Fe} as a function of the reaction time t at various initial NO_2-concentrations: $[NO_2]$ is expressed in units of 10^{11} molecules cm^{-3}; temperature of the solid $FeCl_3$(s) $T_s = 391$ K; reactor pressure P_r 1.3×10^3 Pa argon; gas temperature $T_g = 303$ K. A blank run was performed at the beginning (□) and at the end (●) of the experiment.

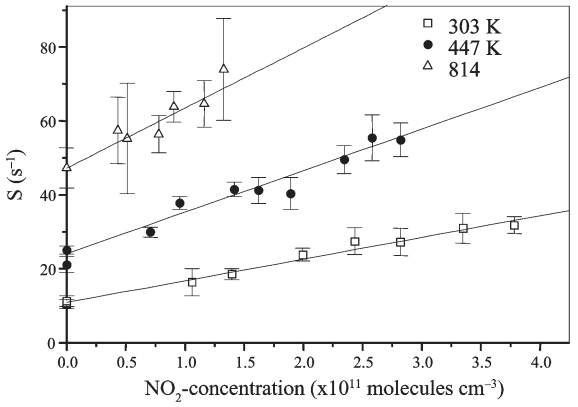

Fig. 2 The observed slope S of eqn. (2) plotted against $[NO_2]$ at gas temperatures $T_g = 303$, 447 and 814 K.

expressed in 10^{-11} cm^3 molecule^{-1} s^{-1}. This indicates that a doubling of hydrogen concentration yields rate constants varying within each error margin. It should be pointed out here that the dissociation yield of hydrogen in argon carrier gas was very low and only of the order of 0.2%. Taking into account that the hydrogen atoms were lost on the reactor wall at a rate of 150 s^{-1}, one can calculate that in the kinetic zone 15 cm or 46 ms downstream of the atomisation region, their concentration becomes totally negligible.

An increase of the reactor pressure P_r from 0.8×10^3 Pa to 1.6×10^3 Pa should result in a decrease by a factor of two of the diffusion coefficient of the reagents and of all relevant intermediates involved. This will have an effect on both the mixing conditions and the loss rate of the Fe atoms on the reactor wall. Within this pressure variation none of these effects seemed to influence the value of k_1 in a systematic way.

Temperature dependence of k_1

The same procedure as described above was now followed for determining k_1 at various temperatures. A summary of the experimental conditions and derived values for k_1 is given in Table 3 for temperatures between 303 and 814 K.

Our data, fitted according to the $\ln k_1$ *versus* $1/T$ weighted linear regression model, yields the expression:

$$k_1 = \left(4.8^{+0.7}_{-0.6}\right) \times 10^{-10} \times \exp\left(\frac{(-4.5 \pm 0.4)\text{kJ mol}^{-1}}{RT}\right) \text{cm}^3 \text{ molecule}^{-1} \text{ s}^{-1} \quad (3)$$

The only other determination of k_1 has been carried out by Plane *et al.*[10] using the pulsed laser photolysis fluorescence-laser induced fluorescence (PLP-LIF) technique. The Fe atoms were produced by pulsed multiphoton photolysis of ferrocene

Table 1 Influence of the salt temperature T_s and hydrogen content on k_1 at 303 K; the reactor pressure $P_r = 1.7 \times 10^3$ Pa

T_s/K	$P_{H_2} \times 10^{-1}$/Pa	$k_1 \times 10^{11}$/cm^3 molecule^{-1} s^{-1}
384	3.1	8.1 ± 1.2
395	3.1	6.2 ± 1.0
413	3.1	6.6 ± 1.1
418	3.1	6.9 ± 1.6
384	6.0	4.4 ± 0.9
389	6.0	5.4 ± 1.1
391	6.0	7.1 ± 2.1
396	6.0	6.2 ± 1.2
402	6.0	7.6 ± 1.1
405	6.0	8.3 ± 1.2

Table 2 Influence of the reactor pressure on k_1 at 303 K; $[H_2] = 6.0 \times 10^{-1}$ Pa

$P_r \times 10^3$/Pa	T_s/K	$k_1 \times 10^{11}$/cm^3 molecule^{-1} s^{-1}
0.8	397	8.5 ± 1.2
0.9	403	7.7 ± 1.0
1.1	395	6.3 ± 1.2
1.2	405	8.0 ± 1.3
1.3	391	7.1 ± 2.1
1.5	404	9.4 ± 1.4
1.6	398	6.0 ± 2.2

in a concentration of *ca.* 5×10^{12} molecule cm^{-3}. The Fe atom decays were monitored in real time by means of laser induced fluorescence. In the temperature range between 192 and 471 K the following expression was derived:

$$k_1 = \left(4.84^{+1.24}_{-1.1}\right) \times 10^{-10} \times \exp\left(\frac{(-2.60 \pm 0.56)\text{kJ mol}^{-1}}{RT}\right) \text{cm}^3 \text{ molecule}^{-1} \text{ s}^{-1} \quad (4)$$

An Arrhenius plot of our results compared to those of Plane *et al.*[10] is shown in Fig. 3

While the pre-exponential factors of both expressions are nearly the same, Plane *et al.* have found a slightly lower value for the activation energy of 2.60 ± 0.56 kJ mol^{-1} *versus* our value of 4.5 ± 0.4 kJ mol^{-1}. Both values just fall outside each other's error margin when 2σ is taken and this results in a value of k_1 which is a factor of 2.3 lower at 295 K in our study. An explanation for this discrepancy is not readily available.

Reaction mechanism

According to the thermochemical data of r.1, the iron oxides could in principle be formed in several excited states[20,21] (see Table 4). In our fast-flow reactor study no chemiluminescence could be observed which is logical in view of the upper wave length range of 900 nm of the multiplier. The emission from the highest excited D $^5\Delta$ state of FeO is indeed situated at 1000 nm and higher.

In low temperature atomic Fe/NO_2 flames a weak emission was recorded at around 500 to 700 nm[22] but it was not clear from where this emission could originate. A more elaborate discussion on the possible sources of these emissions is already given elsewhere.[10]

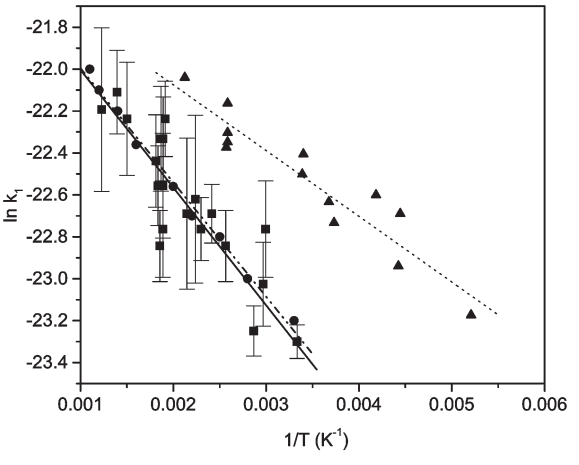

Fig. 3 Arrhenius plot for k_1: this work, eqn. (3) (■,—), the 303 K values are pooled into the weighted average of $(7.4 \pm 0.6) \times 10^{-11}$ cm^3 molecule^{-1} s^{-1}; the gas kinetic collision rate constant k_{col} given by eqn. (6) (●,–·–) and the results of Plane *et al.*,[10] eqn. (5) (▲,···).

Table 3 Experimental conditions and derived values of k_1 as a function of the gas temperature T_g

T_g/K	T/K	$P_r \times 10^3$/Pa	$P_{H_2} \times 10^{-1}$/Pa	$k_1 \times 10^{-11}$/cm^3 molecule^{-1} s^{-1}
303	391	0.8	3.1	7.2 ± 1.3
303	397	0.8	6.0	8.5 ± 1.2
303	391	0.9	3.1	6.4 ± 1.1
303	405	0.9	6.0	7.7 ± 1.0
303	390	1.1	3.3	9.7 ± 1.6
303	393	1.1	3.3	8.0 ± 1.3
303	395	1.1	6.0	6.3 ± 1.2
303	405	1.2	6.0	8.0 ± 1.3
303	384	1.3	3.1	8.1 ± 1.2
303	391	1.3	3.1	9.3 ± 1.6
303	391	1.3	6.0	7.1 ± 2.1
303	395	1.3	3.1	6.2 ± 1.0
303	396	1.3	6.0	6.2 ± 1.2
303	402	1.3	6.0	7.6 ± 1.1
303	405	1.3	6.0	8.3 ± 1.2
303	413	1.3	3.1	6.6 ± 1.1
303	418	1.3	3.1	6.9 ± 1.6
303	404	1.5	6.0	9.4 ± 1.4
303	398	1.6	6.0	6.0 ± 2.2
320	394	1.3	3.1	14 ± 3
334	389	1.3	3.9	13 ± 2
337	389	1.3	6.0	10 ± 2
349	381	1.3	6.0	8 ± 1
390	389	1.3	6.0	12 ± 2
414	400	1.2	6.0	14 ± 2
435	404	1.3	6.0	13 ± 2
447	395	1.3	6.0	15 ± 6
466	392	1.3	6.0	14 ± 5
523	396	1.2	10	22 ± 4
529	396	1.1	10	20 ± 4
530	395	1.6	10	13 ± 3
530	396	0.9	10	16 ± 4
536	400	1.3	10	20 ± 5
539	394	1.3	6.0	12 ± 2
545	396	1.1	10	16 ± 3
552	392	1.2	10	18 ± 4
666	392	1.2	10	22 ± 6
718	395	1.3	10	25 ± 5
814	407	1.3	10	23 ± 9

In analogy with a number of alkaline earth metal/NO_2 reactions,[23] it is interesting to check whether the reaction might proceed according to the "electron jump" mechanism.[11] The Fe atom throws out its valence electron which is then captured by the NO_2 molecule. The distance r_c where the covalent potential energy surface of the two approaching Fe and NO_2 species crosses the Coulombic attraction curve of the Fe^+ and NO_2^- ions is given by[11]

$$e^2/r_c = \mathrm{IE(Fe)} - \mathrm{EA_v(NO_2)} \qquad (5)$$

where e is the electronic charge, IE(Fe) the ionisation energy of the Fe atom and $EA_v(NO_2)$ the vertical electron affinity of NO_2. The ionisation energy of the Fe atom is 7.87 eV and the vertical electron affinity of NO_2 is 1.43 eV.[24] From eqn. (5) the value of $r_c = 2.2$ Å is obtained. It has been suggested that the true value for r_c should be calculated with a value in between the vertical and the adiabatic electron affinity EA_a.[25] Assuming the value of 1.85 eV which is the average between $EA_a(NO_2) = 2.27$ eV[26] and 1.43 eV, one finds only a marginally higher r_c value of 2.38 Å. Given this relatively short distance and taking into account that the reaction shows a small activation energy, one should conclude that the concept of "harpooning" is not applicable to reaction (1).

Table 4 Reaction enthalpies of the reaction of Fe(a^5D_4) atoms with NO_2 forming FeO_g in different electronically excited states

FeO_g	$\Delta H_{298\ K}$/kJ mol^{-1}
X $^5\Delta$	−108.1
a $^7\Sigma+$	−106.3
A $^5\Sigma+$	−60.8
B $^5\Phi$	+10.3
C $^5\Pi$	+10.6
D $^5\Delta$	+112.8

An alternative route is the simple gas kinetic approach, where the rate constant can be calculated from the collision frequency:

$$k_{col} = (\sigma_{A-B})^2 \pi v_r \exp\left(\frac{-E}{RT}\right) \qquad (6)$$

where $\sigma_{A-B} = (\sigma_{Fe} + \sigma_{NO_2})/2$ is the collision diameter and v_r the average molecular speed $(8RT/\pi\mu)^{0.5}$ with μ being the reduced mass of the reagents. The value of σ_{Fe} is taken equal to 3.44 Å[27] and σ_{NO_2} has been approximated by $\sigma_{CO_2} \approx 4$ Å.[28] The exponent E in eqn. (6) is the activation barrier which can be derived from the Arrhenius activation energy E_a with the formula $E = E_a - nRT_{av}$. With $n = 0.5$ and $T_{av} = (T_1T_2)^{0.5}$ where T_1 and T_2 are, respectively, the lowest and highest temperature of the measurements,[29] one obtains the value of the activation barrier $E = 2.3$ kJ mol^{-1}. The logarithm of k_{col} is also plotted in Fig. 3 and one sees an excellent agreement with the experimental values indicating that the steric factor is close to unity, *i.e.* there is no preferred direction of approach.

From his *ab initio* calculations Stirling[30] concluded that the reaction is initiated by an electron transfer from the metal to the NO_2 molecule. This results in weakening of the N–O bond and enhances an $O^-(^2P)$ abstraction. First a bent oxo-nitrosyl insertion complex ON–FeO is formed involving an electron transfer to the LUMO of the NO_2.[30] According to the electronic configuration of the NO_2 molecule which is a $\ldots(5a_1)^2(1b_1)^2(1a_2)^2(4b_2)^2(6a_1)^1$, the HOMO is the single occupied $6a_1$-orbital.[31] It is a π-orbital in plane which is anti-bonding for both NO-bonds. The LUMO corresponds to the $2b_1$-orbital and is also anti-bonding for both bonds. The ground state NO_2^--ion ($^1A1$) is formed when the electron comes into the single occupied $6a_1$ orbital and this is a very exothermic process yielding an electron affinity of +2.27 eV.[26] However, when the electron accommodates in the LUMO, the NO_2^--ion is formed in an excited state $^3B1$ or $^1B1$ which lie, respectively, 3 and 3.8 eV above the ground state.[32,33] In this way the charge transfer reaction becomes endothermic and the vertical electron affinity EA_v decreases to −0.57 and −1.23 eV for the respective $^3B1$ and $^1B1$ states. Most probably, the 4s electron of the iron atom will rather be transferred to the HOMO instead of the LUMO. On the basis of D.F.T. calculations on the Cu + NO_2 reaction where a planar complex was formed by a 4s electron transfer from the Cu atom into the $6a_1$ orbital of NO_2,[34,35] an analogous behaviour for the Fe + NO_2 reaction can be expected.

In a further step the final products will be formed according to reactions (4) to (5):

$$NO_2^- (^1A1) \rightarrow NO\ (^2\Pi) + O^-\ (^2P) \qquad (r.4)$$

$$Fe^+(^6D) + O^-(^2P) \rightarrow FeO\ (X\ ^5\Delta) \qquad (r.5)$$

From this sequence it becomes clear that the N–O bond breaking and the FeO formation processes occur along spin-conservation routes which is a necessary condition for achieving high Arrhenius pre-exponential factors nearly equal to the collision frequency. The reaction proceeds by crossing a barrier but its height doesn't exceed the energy of the reagents. This implies that a small activation energy of a few kJ mol^{-1}

is very reasonable. Taking the arguments given above into account it is also logical that Stirling called his mechanism an "electron-transfer-assisted oxygen abstraction.[30]

Acknowledgements

The authors thank the Flemish Fund for Scientific Research (FWO-Vlaanderen) for a research grant.

References

1 A. Fontijn and W. Felder, in *Reactive Intermediates in the Gas Phase, Generation and Monitoring*, ed. D. W. Setser, Academic Press, New York, 1979, ch. 2.
2 P. Marshall, A. S. Narayan and A. Fontijn, *J. Phys. Chem.*, 1990, **94**, 2998.
3 M. Helmer and J. M. C. Plane, *J. Chem. Soc., Faraday Trans.*, 1994, **90**, 31.
4 M. Helmer and J. M. C. Plane, *J. Chem. Soc., Faraday Trans.*, 1994, **90**, 395.
5 M. Campbell and J. R. Metzger, *Chem. Phys. Lett.*, 1996, **253**, 158.
6 S. A. Mitchell and P. H. Hackett, *J. Chem. Phys.*, 1990, **93**, 7813and ibid. 7822.
7 D. Ritter and J. C. Weisshaar, *J. Am. Chem. Soc.*, 1990, **112**, 6425.
8 C. Vinckier, A. Dumoulin, J. Corthouts and S. De Jaegere, *J. Chem. Soc., Faraday Trans. 2*, 1988, **84**, 1725.
9 C. Vinckier, K. Cappan, *ChemPhysChem*, 2003, in press.
10 J. M. C. Plane and R. J. Rollason, *Phys. Chem. Chem. Phys.*, 1999, **1**, 1843.
11 D. R. Herscbach, *Adv. Chem. Phys.*, 1966, **10**, 319.
12 C. Vinckier, T. Verhaeghe and I. Vanhees, *J. Chem. Soc., Faraday Trans. 2*, 1994, **90**, 2003.
13 C. Vinckier and I. Vanhees, *J. Phys. Chem.*, 1998, **102**, 1349.
14 C. L. Talcott, J. W. Ager and C. J. Howard, *J. Chem. Phys.*, 1986, **84**, 6161.
15 J. A. Silver, *J. Chem. Phys.*, 1984, **81**, 5125.
16 R. W. Huggins and J. H. Cahn, *J. Appl. Phys.*, 1967, **38**, 180.
17 C. J. Howard, *J. Phys. Chem.*, 1979, **83**, 3.
18 A. Fontijn and W. Felder, *J. Phys. Chem.*, 1979, **83**, 24.
19 *SAS statistical package*, SAS Institute Inc., Cary, NC, 1992.
20 J. Sugar and C. Corliss, *J. Phys. Chem. Ref. Data*, 1985, **14**(2), 407.
21 A. J. Merer, *Annu. Rev. Phys. Chem.*, 1989, **40**, 407.
22 J. B. West and H. P. Broida, *J. Chem. Phys.*, 1975, **62**, 2566.
23 C. Vinckier, J. Helaers, P. Christiaens and J. Remeysen, *J. Phys. Chem. A*, 1999, **103**, 11 322.
24 E. Andersen and J. Simons, *J. Chem. Phys.*, 1977, **66**, 2427.
25 E. M. Goldfield, A. M. Kosmas and E. A. Gislason, *J. Chem. Phys.*, 1985, **82**, 3191.
26 K. M. Ervin, J. Ho and W. C. Lineberger, *J. Phys. Chem.*, 1988, **92**, 5405.
27 D. Ritter, J. J. Carroll and J. C. Weisshaar, *J. Phys. Chem.*, 1992, **96**, 10 636.
28 J. O. Hirschfelder, C. F. Curtiss and R. B. Bird, *Molecular Theory of Gases and Liquids*, J. Wiley & Sons, New York, 1967, p. 561.
29 P. M. Futerko and A. Fontijn, *J. Chem. Phys.*, 1991, **95**, 8065.
30 A. Stirling, *J. Am. Chem. Soc.*, 2002, **124**, 4058.
31 G. Herzberg, *Molecular Spectra and Molecular Structure III: Electronic Spectra and Electronic Structures of Poly-atomic Molecules*, Krieger Publ. Comp., Florida, 1991, p. 345.
32 P. A. Benioff, *J. Chem. Phys.*, 1978, **68**, 3405.
33 Z. L. Cai, *J. Chem. Soc., Faraday Trans.*, 1993, **89**, 991.
34 L. Rodrigez-Santiago, V. Branchadell and M. Sodupe, *J. Chem. Phys.*, 1995, **103**, 9738.
35 L. Rodrigez-Santiago, M. Sodupe and V. Branchadell, *J. Chem. Phys.*, 1996, **105**, 9966.